

## Equation of state of a high-pressure phase of $\text{Gd}_3\text{Ga}_5\text{O}_{12}$

Z. Mao,<sup>1,2</sup> S. M. Dorfman,<sup>1</sup> S. R. Shieh,<sup>3</sup> J. F. Lin,<sup>2</sup> V. B. Prakapenka,<sup>4</sup> Y. Meng,<sup>5</sup> and T. S. Duffy<sup>1</sup>

<sup>1</sup>*Department of Geosciences, Princeton University, Princeton, New Jersey 08544, USA*

<sup>2</sup>*Department of Geological Sciences, Jackson School of Geosciences, The University of Texas at Austin, Austin, Texas 78712, USA*

<sup>3</sup>*Department of Earth Sciences, Physics, and Astronomy, University of Western Ontario, London, Ontario N6A 5B7, Canada*

<sup>4</sup>*Consortium for Advanced Radiation Sources (CARS), University of Chicago, Argonne National Laboratory, Argonne, Illinois 60439, USA*

<sup>5</sup>*HPCAT, Carnegie Institution of Washington, Argonne, Illinois 60439, USA*

(Received 3 November 2010; revised manuscript received 3 January 2011; published 24 February 2011)

$\text{Gd}_3\text{Ga}_5\text{O}_{12}$  (GGG), which crystallizes in the garnet structure at ambient conditions, was observed to transform to a high-pressure phase at 88 GPa after laser heating at 1500 K. This new phase is stable at least up to 180 GPa, and can be preserved on decompression to 50 GPa. This phase is cubic and consistent with a perovskite structure of stoichiometry  $(\text{Gd}_{0.75}\text{Ga}_{0.25})\text{GaO}_3$ . The zero-pressure bulk modulus,  $K_0$ , obtained from fitting to a Birch-Murnaghan equation of state is 373(5) GPa with a fixed pressure derivative  $K'_0 = 4$ . At 170 GPa, the bulk modulus of perovskite-type GGG is 979(15) GPa, which is comparable to that of diamond at the same pressure [956(21) GPa] and consistent with recently reported shock-compression data for  $\text{Gd}_3\text{Ga}_5\text{O}_{12}$ . The new high-pressure phase of  $\text{Gd}_3\text{Ga}_5\text{O}_{12}$  is thus highly incompressible.

DOI: [10.1103/PhysRevB.83.054114](https://doi.org/10.1103/PhysRevB.83.054114)

PACS number(s): 64.30.Jk, 61.05.cf, 62.50.-p, 91.60.Ba

### I. INTRODUCTION

Shock-compression experiments have reported that gadolinium gallium garnet,  $\text{Gd}_3\text{Ga}_5\text{O}_{12}$ , (GGG) transforms to a highly incompressible phase that is stiffer than shock-compressed sapphire or diamond above 170 GPa.<sup>1</sup> This finding has practical relevance for shock experiments on metallic hydrogen and other highly compressible materials that rely on shock reverberations between incompressible disks to achieve high pressures (up to  $\sim 300$  GPa).<sup>2</sup> More generally, this discovery suggests that oxide phases formed from rare-earth garnets may have interesting properties at high pressures and are candidates for highly incompressible solids.

Rare-earth oxide garnets (space group  $Ia3d$ ) have the general chemical formula  $\text{A}_3\text{B}_5\text{O}_{12}$ , where A is  $\text{Y}^{3+}$  or a rare earth cation such as  $\text{Gd}^{3+}$  and B is  $\text{Al}^{3+}$ ,  $\text{Ga}^{3+}$ , or  $\text{Fe}^{3+}$ . These garnets have a variety of technical applications such as solid-state laser crystals, phosphors, ionic conductors, and magneto-optic devices.<sup>3,4</sup> With suitable dopants, they can serve as optical pressure sensors at high pressures (e.g., Sm-doped yttrium aluminum garnet).<sup>5</sup> GGG has also been investigated as an anvil material for dynamic loading of precompressed samples.<sup>6</sup> High-temperature creep properties of these materials have been of interest to geoscientists studying deformation mechanisms in garnets.<sup>7,8</sup>

A number of high-pressure experiments have been performed on GGG and other rare-earth garnets. Based on high-pressure diamond anvil cell (DAC) experiments at room temperature, GGG was found to remain in the garnet structure until it became amorphous above 84 GPa.<sup>9</sup> Pressure-induced amorphization has also been observed at room temperature in  $\text{Gd}_3\text{Sc}_2\text{Ga}_3\text{O}_{12}$  (GSGG) at 58 GPa<sup>9</sup> and  $\text{Y}_3\text{Fe}_5\text{O}_{12}$  (YIG) at 50 GPa.<sup>10</sup> Recently, the high-pressure equation of state of GGG was investigated in diamond anvil cell experiments (to 25 GPa) and density functional theory calculations.<sup>11</sup> A number of high-pressure spectroscopic studies and lattice dynamics calculations on rare-earth oxide garnets have also been performed to investigate their structure and thermodynamic properties at high pressures.<sup>12-15</sup>

Shock-compression experiments<sup>1,16</sup> on GGG up to 260 GPa show that the Hugoniot elastic limit of GGG is approximately 30 GPa. Pressure-volume compression data were interpreted as a continuous phase transition occurring over 65–120 GPa and a quasi-incompressible phase stable above 120 GPa.<sup>1,16</sup> The Hugoniot compression curve for the high-pressure phase becomes stiffer than that of diamond above 170 GPa. Electrical conductivity measurements indicate that the high-pressure phase is a semiconductor with a band gap of 3.1 eV.

In the shock-wave experiments, the structure of the high-pressure phase could not be determined. Moreover, none of the static diamond cell experiments to date have reached the high-pressure conditions of the shock experiments nor was used heating to promote phase transitions under compression. In this study, we use the laser-heated diamond anvil cell and synchrotron x-ray diffraction to investigate the phase stability and elastic properties of GGG to 180 GPa. We focus mainly on exploring the high-pressure phase of GGG, constraining the phase boundary and determining the equation of state and crystal structure of the new phase.

### II. EXPERIMENTAL DETAILS

Single-crystal GGG (from MTI corporation and Princeton Scientific Corporation) was ground into fine powder. The starting sample was examined by x-ray diffraction and Raman spectroscopy, and confirmed to be in the garnet structure with no other phases detected. The lattice parameter at 1 bar and room temperature was 12.3796(6) Å, consistent with previous reports for a pure GGG phase.<sup>1,11</sup> High-pressure experiments were carried out using a symmetric DAC. The powder sample was mixed with 10 wt% Pt, which served as a pressure calibrant and laser absorber. The mixture was compressed into a  $\sim 7$ - $\mu\text{m}$ -thick foil and loaded into the DAC sample chamber. For measurements up to 90 GPa, a cell with 200  $\mu\text{m}$  culet anvils was used. To provide a quasihydrostatic environment and a better thermal insulation during laser heating, neon was loaded into the cell using the COMPRES/GSECARS system.<sup>17</sup>

A  $\sim 3\text{-}\mu\text{m}$ -thick GGG foil without Pt was placed below the sample foil to allow the neon medium to flow in. The second sample was loaded into a cell with two beveled diamond anvils ( $75\text{-}\mu\text{m}$  inner culet and  $300\text{-}\mu\text{m}$  outer culet) for measurements above 90 GPa. This sample was sandwiched between two NaCl foils, which acted as the pressure medium and thermal insulation layers. In both experiments, rhenium gaskets were preindented to  $\sim 25\text{-}\mu\text{m}$  thickness, and were drilled to a 100- or  $25\text{-}\mu\text{m}$ -diameter hole serving as sample chambers.

High-pressure angle-dispersive x-ray diffraction experiments were carried out at 13-ID-D of the GSECARS sector and 16-ID-B of the HPCAT sector at the Advanced Photon Source, Argonne National Laboratory. A monochromatic beam was focused to a size of  $\sim 5 \times 7\text{-}\mu\text{m}^2$  on the sample. All diffraction patterns were collected using a CCD detector that was calibrated with a  $\text{CeO}_2$  standard. Pressure was determined based on the equation of state of Pt.<sup>18</sup> We initially compressed the sample at ambient temperature to 86 GPa and then laser heated the sample from both sides to approximately 1500 K. X-ray diffraction patterns of GGG were collected every 10 to 15 GPa up to 180 GPa. The sample was heated at each pressure step to between 1500 and 1800 K for at least 30 minutes.

### III. RESULTS AND DISCUSSION

The cubic garnet phase was found to be stable up to 70 GPa. GGG became partially amorphous at 80 GPa, and completely amorphous at 86 GPa, consistent with previous work.<sup>9</sup> The amorphous GGG immediately transformed into a new high-pressure phase at 88 GPa upon laser heating to 1500 K. In total, we observed nine diffraction peaks for the high-pressure phase. No difference in the x-ray diffraction pattern was observed under *in situ* high pressure-temperature conditions and upon temperature quench. The program DICVOL was used to identify candidate unit cells for the new structure.<sup>19</sup> The new phase can be indexed as a cubic phase that is consistent with a perovskite structure (Fig. 1). According to the stoichiometry

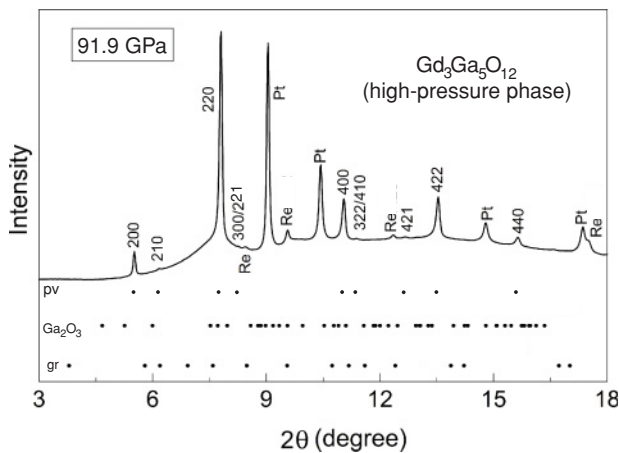


FIG. 1. Angle-dispersive x-ray diffraction pattern (wavelength  $\lambda = 0.3344\text{ \AA}$ ) of high-pressure  $\text{Gd}_3\text{Ga}_5\text{O}_{12}$  phase (Pv) indexed to a cubic unit cell. Tick marks show expected peak locations for  $\text{Gd}_3\text{Ga}_5\text{O}_{12}$  garnet (gr) and  $\text{Ga}_2\text{O}_3$  in  $\text{Rh}_2\text{O}_3$  (II) type structure at 91.9 GPa.<sup>21</sup> Re peaks are from gasket due to incomplete filtering x-ray beam tails.

TABLE I. Observed x-ray diffraction peaks of high-pressure  $\text{Gd}_3\text{Ga}_5\text{O}_{12}$  phase at 91.9 GPa and 300 K. The structure is refined using cubic symmetry with  $a = 6.953(1)\text{ \AA}$ . Wavelength  $\lambda = 0.3344\text{ \AA}$ .

$hkl$	$2\theta$ (degree)	$d_{\text{obs}}$ ( $\text{\AA}$ )	$d_{\text{calc}}$ ( $\text{\AA}$ )	$d_{\text{obs}}/d_{\text{calc}} - 1$	$I_{\text{obs}}/I_0$
200	5.5172	3.4740	3.4763	-0.0006	9
210	6.1673	3.1082	3.1093	-0.0004	<1
220	7.7985	2.4588	2.4581	0.0003	100
300	8.2612	2.3213	2.3175	0.0016	<1
221	8.2612	2.3213	2.3175	0.0016	<1
400	11.0435	1.7376	1.7381	-0.0003	21
322	11.3895	1.6850	1.6862	-0.0007	<1
410	11.3895	1.6850	1.6862	-0.0007	<1
421	12.6686	1.5155	1.5172	-0.0011	<1
422	13.5341	1.4190	1.4192	-0.0002	16
440	15.6373	1.2291	1.2291	0.0000	3

of GGG, the formula for the cubic perovskite phase should be  $(\text{Gd}_{0.75}\text{Ga}_{0.25})\text{GaO}_3$ , implying that the high-pressure phase is an A-site ordered double perovskite. Table I compares the position of the observed diffraction peaks with the fit to a cubic unit cell at 91.9 GPa and 300 K. Lattice parameters and the corresponding unit cell volumes at each pressure are listed in Table II.

GGG might be expected to decompose into  $\text{GdGaO}_3$  perovskite plus the high-pressure phase of  $\text{Ga}_2\text{O}_3$ .<sup>20</sup> However, comparing the diffraction peak positions of  $\text{Ga}_2\text{O}_3$  in  $\text{Rh}_2\text{O}_3$  (II) type structure at  $\sim 92$  GPa to our high-pressure GGG (Fig. 1) shows that the obtained high-pressure phase could not be explained as a mixture of  $\text{GdGaO}_3$  and  $\text{Ga}_2\text{O}_3$ .<sup>21</sup> No additional phase transitions were observed up to 180 GPa. Figure 2 shows the representative diffraction patterns of GGG collected at different pressures. The Hugoniot temperature for GGG at 120 GPa is calculated to be  $\sim 1000$  K (T. Mashimo, personal communication), so our temperature range is comparable to or above the shock experiments. Upon heating over 2000 K, we sometimes observed some

TABLE II. Lattice parameter and volume of the high-pressure phase of  $\text{Gd}_3\text{Ga}_5\text{O}_{12}$  at each pressure

	P (GPa)	$a$ ( $\text{\AA}$ )	$V$ ( $\text{\AA}^3$ )
Compression	91.9(5)	6.9527(10)	336.1(1)
	109.5(7)	6.9139(17)	330.5(2)
	118.8(8)	6.8901(19)	327.1(3)
	129.2(9)	6.8563(13)	322.3(2)
	140.4(9)	6.8299(22)	318.6(3)
	145.3(10)	6.8127(31)	316.2(4)
	156.9(9)	6.7860(26)	312.5(4)
	163.7(9)	6.7708(29)	310.4(4)
177.1(10)	6.7306(53)	304.9(7)	
Decompression	50.4(7)	7.1328(7)	362.9(1)
	69.4(6)	7.0407(26)	349.0(4)
	74.9(8)	7.0189(17)	345.8(3)
	80.9(10)	7.0115(28)	344.7(4)
	87.0(13)	6.9879(30)	341.2(4)
	88.5(3)	6.9644(45)	337.8(7)

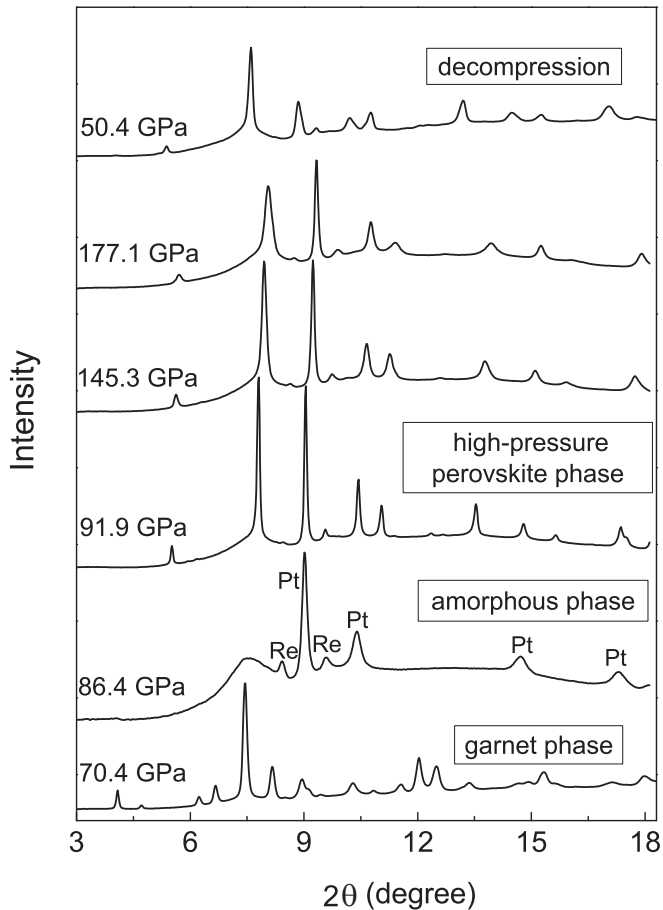


FIG. 2. Representative angle-dispersive x-ray diffraction patterns of GGG.

additional peak splittings suggesting structural distortion and/or chemical reaction with other components of the sample assemblage. This will be the subject of further investigation. Decompressing the cell at ambient temperature showed that the high-pressure phase remained stable at least down to 50 GPa. Upon further decompression, the pressure suddenly dropped to 1 bar, and the sample could not be recovered.

A third-order Birch-Murnaghan equation of state was used to fit the measured pressure-volume (P-V) data for the high-pressure perovskite phase of GGG (Fig. 3). Using both compression and decompression results in the fitting, the bulk modulus,  $K_0$ , obtained is 373(5) GPa with  $V_0 = 402.0(7) \text{ \AA}^3$  and  $K'_0 = 4.0$  (fixed) or 392(26) GPa with  $V_0 = 400.3(21) \text{ \AA}^3$  and  $K'_0 = 3.8(3)$ . By only using the compression data, fitting the P-V relations yields  $V_0 = 395.8(12) \text{ \AA}^3$  and  $K_0 = 414(9) \text{ GPa}$  with fixed  $K'_0 = 4.0$ . The uncertainty in  $K_0$  and  $V_0$  is likely underestimated due to the fixed value of  $K'_0$ . We varied the fixed value of  $K'_0$  from 3.5 to 4.5, and found that  $K_0$  and  $V_0$  varied by  $\pm 46 \text{ GPa}$  and  $\pm 3.9 \text{ \AA}^3$  over this range. The equation of state results also can depend on the choice of the Pt equation of state.<sup>18,22</sup> Using the equation of state of Ref. 22 instead of Ref. 18 for fixed  $K'_0$  results in a  $K_0$  value that is lower by  $\sim 15\%$  and a  $V_0$  value that is larger by 1.6%. We also evaluated the differential stress in our samples using the diffraction peaks

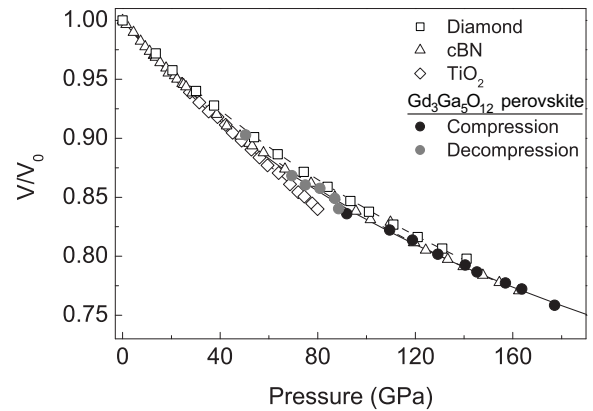


FIG. 3. Equation of state of high-pressure phase of GGG. Black solid circle: high-pressure  $\text{Gd}_3\text{Ga}_5\text{O}_{12}$  phase in compression; gray solid circle: high-pressure phase of GGG in decompression; open square: diamond (Ref. 27); open triangle: cubic boron nitride (cBN) (Ref. 28); open diamond:  $\text{TiO}_2$  in the cotunnite ( $\text{PbCl}_2$ ) structure (Ref. 29); solid lines: a fit to the P-V relations of GGG using the Birch-Murnaghan equation of state; dashed lines: a fit to the P-V relations of diamond, cubic boron nitride, and  $\text{TiO}_2$ .

111 and 200 of Pt pressure standard.<sup>23–25</sup> From 90 to 177 GPa, the product of differential stress  $t$  and elastic anisotropy factor  $S$  ranges from 0.0016 to 0.0026 after laser annealing. The corresponding differential stress according to Ref. 26 is less than 1 GPa.

In Fig. 3, we compare the P-V relations of GGG with selected highly incompressible materials: diamond,<sup>27</sup> cubic boron nitride,<sup>28</sup> and  $\text{TiO}_2$  in the cotunnite ( $\text{PbCl}_2$ -type) structure.<sup>29</sup> With increasing pressure, the perovskite phase of  $\text{Gd}_3\text{Ga}_5\text{O}_{12}$  is slightly more compressible than diamond, comparable to cubic boron nitride, but is stiffer than  $\text{TiO}_2$ . In Ref. 1, it was found that GGG becomes more incompressible than diamond above 170 GPa under shock-wave loading. Here, our calculated bulk modulus for the high-pressure phase of GGG at 170 GPa is 979(15) GPa, which is indistinguishable from that of diamond [956(21) GPa] at this pressure.<sup>27</sup> In the shock-compression study, Hugoniot data were reported to 260 GPa.<sup>1</sup> At low pressures, the Hugoniot is consistent with static data for the garnet phase. Since shock temperatures are low below 65 GPa, the thermal pressure is small and the shock and static data are directly comparable. At 65–120 GPa, the Hugoniot data are interpreted as indicating a broad phase transition interval (a mixed phase region). The Hugoniot of the high-pressure phase above 120 GPa is quasi-incompressible and stiffer than the Hugoniot of diamond above 170 GPa. Electrical conductivity measurements show that the high-pressure phase remains an insulator with a significant band gap. The reduced shock isotherm yields the following parameters:  $\rho_0 = 9.32 \text{ g/cm}^3$ ,  $K_0 = 440(6) \text{ GPa}$ , and  $K'_0 = 4.8(3)$ .

In order to facilitate comparison with shock data, we plot our data and other recent studies as pressure versus density in Fig. 4 assuming two formula units per cell ( $Z = 2$ ) for the high-pressure GGG phase.<sup>1,9,11</sup> For the cubic garnet phase, our data are consistent with low-pressure Hugoniot data and other

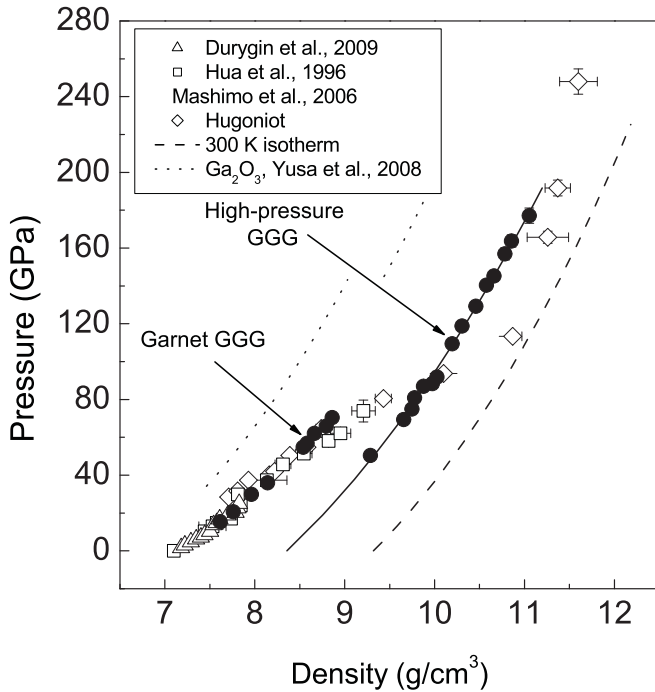


FIG. 4. Comparison of the density-pressure relationships of GGG in this study to results from Refs. 1, 9, and 11. Solid circle and line: this study; open square: from Ref. 9; open triangle: Ref. 11; open diamond: from Ref. 1; dashed line: 300 K reduced isotherm from shock-wave experiments;<sup>1</sup> dotted line:  $\text{Ga}_2\text{O}_3$  in  $\text{Rh}_2\text{O}_3$  (II) type structure and *Cmcm* structure Refs. 21 and 40.

static compression studies.<sup>1,9,11</sup> In detail, there are differences between the static compression studies that are most likely due to different degrees of nonhydrostatic stress as the samples were not annealed in this compression range. The zero-pressure bulk modulus of the perovskite phase of  $\text{Ga}_3\text{Gd}_5\text{O}_{12}$  (373 GPa) can be compared to those of other incompressible materials such as diamond (442 GPa),<sup>27</sup> osmium (395–463 GPa),<sup>30,31</sup> cubic boron nitride (367 GPa),<sup>28</sup> and sapphire (250 GPa). Other highly incompressible materials that have been recently identified from static compression experiments include cotunnite-type  $\text{TiO}_2$  (431 GPa),<sup>32</sup> and transition metal diborides such as  $\text{ReB}_2$  (360 GPa).<sup>33</sup> However, reports of highly incompressible materials are often controversial because of use of different pressure medium or lack of laser annealing. For example, more recent studies of the cotunnite-type phase of  $\text{TiO}_2$  have reported much lower bulk moduli ( $\sim 300$  GPa) for this phase.<sup>34</sup>

There are a number of factors that must be considered when evaluating bulk moduli from static compression experiments. Due to the tradeoffs with  $V_0$  and  $K'_0$ , our bulk modulus has uncertainty that could be estimated to be about  $\pm 10\%$ . In addition, the presence of residual differential stresses in high-pressure diamond anvil cell experiments can lead to serious overestimation of the bulk modulus.<sup>35</sup> As discussed above, our experiments were conducted in quasihydrostatic media and laser annealed at each compression step, and there was no evidence for systematic lattice parameter differences indicative of differential stress. Note also that many reports of very high  $K_0$  values are coupled with very low  $K'_0$  values,

thus maximizing the fit value of  $K_0$  for a particular equation of state. We have used a fixed  $K'_0$  of 4 to avoid this type of potential bias. In addition, we have also made a direct calculation of the bulk modulus at high pressures to avoid some of the uncertainties associated with extrapolation back to ambient pressure.

Despite the uncertainties associated with determination of compressibility at such extreme conditions, our results do indicate that the high-pressure perovskite phase observed here warrants further examination as a highly incompressible material. This is supported by the independent shock- and static-compression studies for this material, which each find evidence for a highly incompressible phase. Note that the finding from shock data that the high-pressure phase of GGG is stiffer than diamond is based on a direct comparison of the measured Hugoniot of both materials, and does not depend on the uncertain reduction of the shock data to a static isotherm.<sup>1</sup>

For the high-pressure phase of GGG, our densities are close to the directly measured Hugoniot points. If the shock datum at 113 GPa is neglected, then the Hugoniot curve and our measured 300-K compression curve would be nearly coincident. However, our data are offset by  $\sim 0.8$  g/cm<sup>3</sup> to a lower value from the 300-K isotherm inferred from the shock-wave data (Fig. 4). The reduction of shock-compression data to an isotherm for a material undergoing a phase transformation requires a number of assumptions and has considerable uncertainty associated with it, so a comparison with direct Hugoniot data may be more meaningful in this case. For  $\text{Al}_2\text{O}_3$ , it has recently been shown that the shock-compression curve and 300 K isotherm are virtually identical up to 400 GPa,<sup>36</sup> similar to what we observe for GGG. The  $\text{Al}_2\text{O}_3$  results were associated with dissipative energy going mostly not into heating the material, but instead concentrated in entropy production.<sup>36</sup>

Since the structure of the high-pressure phase in shock-wave studies is not determined, we can not rule out the possibility that the high-pressure phase obtained here is different from that in Ref. 1. For example, the high-pressure phase on shock loading could be a disordered or metastable phase due to the short time scale of shock experiments. In the higher pressure range of the shock data, a liquid phase is also possible. However, such a large density difference between the phase we observe and these other possible phases is still unlikely, and it is more probable that the shock data have been overcorrected in calculating the isotherm. Furthermore, the shock-reduced isotherm for GGG yields a volume (density) change of  $\sim 30\%$  from garnet to the high-pressure phase at 1 bar. This is larger than what has been typically reported in the volume change across the garnet-perovskite transition. For  $\text{MgSiO}_3$ ,  $\text{Mg}_3\text{Al}_2\text{Si}_3\text{O}_{12}$ , and  $\text{Y}_3\text{Fe}_5\text{O}_{12}$ , the garnet-perovskite volume difference at 1 bar ranges from 11%–16%.<sup>37–39</sup> Our derived volume change of 18% for GGG is consistent with expectations for this type of phase transition. At the phase transition pressure (90 GPa), the density change we observe for the phase transition in  $\text{Gd}_3\text{Ga}_5\text{O}_{12}$  is close to 10%.

In conclusion, we have studied the high-pressure phase transition of  $\text{Gd}_3\text{Ga}_5\text{O}_{12}$  using synchrotron x-ray diffraction up to 180 GPa. GGG is stable in the garnet phase from ambient

pressure to 70 GPa at 300 K, and becomes partly and then completely amorphous at 86 GPa. A new high-pressure phase that can be indexed to a cubic cell was synthesized at 88 GPa after laser heating to 1500 K. This new phase matched the cubic perovskite structure and is stable up to 180 GPa. It can be preserved down to at least 50 GPa during decompression. The bulk modulus  $K_0$  and its pressure derivative  $K'_0$  derived from fitting the measured P-V relations are 373(5) GPa and 4(fixed), respectively.

Compared with Hugoniot data for GGG, our results are consistent in that we find that there is a phase transition to a phase with diamond-like compressibility above 90 GPa. However, our 300 K equation of state yields densities lower by  $\sim 20\%$  compared to the reduced shock isotherm. The density change we observe is more consistent with typical values for garnet-perovskite transitions. The difference may be partly due to uncertainties in the shock-reduced isotherm, but the possibility of different phase being achieved by static and shock loading also needs further investigation. Compared with the P-V relations of other super hard materials, the high-pressure phase of  $\text{Gd}_3\text{Ga}_5\text{O}_{12}$  is slightly more compressible than diamond at low pressures, and its bulk modulus is comparable to that of diamond at 170 GPa. The results

reported here reveal that the high-pressure cubic perovskite phase of GGG is a highly incompressible material at pressures above 1 Mbar.

#### ACKNOWLEDGMENTS

We acknowledge I. Kantor for experimental assistance, and W. J. Nellis and T. Mashimo for helpful discussion. This research was partially supported by COMPRES, the Consortium for Materials Property Research in Earth Science, Carnegie/DOE alliance center and by NSF Grant No. EAR-0738510 to T. S. Duffy, and EFree of the Energy Frontier Research Centers and NSF Grant No. EAR-0838221 to J. F. Lin. Portions of this work were performed at GSECARS and HPCAT at APS, ANL. GSECARS is supported by NSF, under Contract No. EAR-0622171 and DOE (Contract No. DE-FG02-94ER14466). HPCAT is supported by DOE-BES, DOE-NNSA, NSF, and the W. M. Keck Foundation. APS is supported by DOE-BES, under Contract No. DE-AC02-06CH11357. Use of the Advanced Photon Source was supported by the US Department of Energy, Office of Science, Office of Basic Energy Sciences, under Contract No. DE-AC02-06CH11357.

- 
- <sup>1</sup>T. Mashimo, R. Chau, Y. Zhang, T. Kobayoshi, T. Sekine, K. Fukuoka, Y. Syono, M. Kodama, and W. J. Nellis, *Phys. Rev. Lett.* **96**, 105504 (2006).
- <sup>2</sup>W. J. Nellis, S. T. Weir, and A. C. Mitchell, *Phys. Rev. B* **59**, 3434 (1999).
- <sup>3</sup>J. E. Geusic, H. M. Marcos, and L. G. V. Uitert, *Appl. Phys. Lett.* **4**, 182 (1964).
- <sup>4</sup>P. Schiffer, A. P. Ramirez, D. A. Huse, P. L. Gammel, U. Yaron, D. J. Bishop, and A. J. Valentino, *Phys. Rev. Lett.* **74**, 2379 (1995).
- <sup>5</sup>J. Liu and Y. K. Vohra, *Appl. Phys. Lett.* **64**, 3386 (1994).
- <sup>6</sup>T. Kimura *et al.*, *J. Phys.: Conf. Ser.* **215**, 012152 (2010).
- <sup>7</sup>S. Karato, Z. Wang, and K. Fujino, *J. Mater. Sci.* **29**, 6458 (1994).
- <sup>8</sup>Z. Wang, S. Karato, and K. Fujino, *Phys. Chem. Miner.* **23**, 73 (1996).
- <sup>9</sup>H. Hua, S. Mirov, and Y. K. Vohra, *Phys. Rev. B* **54**, 6200 (1996).
- <sup>10</sup>A. G. Gavriliuk, V. V. Struzhkin, I. S. Lyubutin, M. I. Erements, I. A. Trojan, and V. V. Artemov, *Pis'ma v ZhETF* **83**, 41 (2006).
- <sup>11</sup>A. Durygin, V. Drozd, W. Paszkowicz, E. Werner-Malento, R. Buczko, A. Kaminska, S. Saxena, and A. Suchocki, *Appl. Phys. Lett.* **95**, 141902 (2009).
- <sup>12</sup>K. Papagelis, J. Arvanitidis, G. Kanellis, S. Ves, and G. A. Kourouklis, *J. Phys. Condens. Matter* **14**, 3875 (2002).
- <sup>13</sup>J. Arvanitidis, K. Papagelis, D. Christofilos, H. Kimura, G. A. Kourouklis, and S. Ves, *Phys. Status Solidi B* **14**, 3149 (2004).
- <sup>14</sup>R. C. Middleton, D. V. S. Muthu, and M. B. Kruger, *Solid State Commun.* **148**, 310 (2008).
- <sup>15</sup>P. Goel, R. Mittal, N. Choudhury, and S. L. Chaplot, *J. Phys. Condens. Matter* **22**, 065401 (2010).
- <sup>16</sup>W. J. Nellis, *J. Phys.: Conf. Ser.* **121**, 062005 (2008).
- <sup>17</sup>M. Rivers, V. B. Prakapenka, A. Kubo, C. Pullins, C. M. Holl, and S. D. Jacobsen, *High Pressure Res.* **28**, 273 (2008).
- <sup>18</sup>N. C. Holmes, J. A. Moriarty, G. R. Gathers, and W. J. Nellis, *J. Appl. Phys.* **66**, 2962 (1989).
- <sup>19</sup>A. Boulitf and D. Louër, *J. Appl. Cryst.* **37**, 724 (2004).
- <sup>20</sup>N. Miyajima, K. Fujino, N. Funamori, T. Kondo, and T. Yagi, *Phys. Earth Planet. Inter.* **116**, 117 (1999).
- <sup>21</sup>H. Yusa, T. Tsuchiya, N. Sata, and Y. Ohishi, *Phys. Rev. B* **77**, 064107 (2008).
- <sup>22</sup>Y. Fei, A. Ricolleau, M. Frank, K. Mibe, G. Shen, and V. B. Prakapenka, *Proc. Natl. Acad. Sci. USA* **104**, 9182 (2007).
- <sup>23</sup>A. K. Singh, *J. Appl. Phys.* **73**, 4278 (1993).
- <sup>24</sup>C. E. Runge, A. Kubo, B. Kiefer, Y. Meng, V. B. Prakapenka, G. Shen, R. J. Cava, and T. S. Duffy, *Phys. Chem. Miner.* **33**, 699 (2006).
- <sup>25</sup>S. M. Dorfman, F. Jiang, Z. Mao, A. Kubo, Y. Meng, V. B. Prakapenka, and T. S. Duffy, *Phys. Rev. B* **81**, 174121 (2010).
- <sup>26</sup>E. Menendez-Proupin and A. K. Sing, *Phys. Rev. B* **76**, 054117 (2007).
- <sup>27</sup>F. Occelli, P. Loubeyre, and R. Letoullec, *Nat. Mater.* **2**, 151 (2003).
- <sup>28</sup>F. Datchi, A. Dewaele, Y. Le Godec, and P. Loubeyre, *Phys. Rev. B* **75**, 214104 (2007).
- <sup>29</sup>R. Ahuja and L. S. Dubrovinsky, *J. Phys. Condens. Matter* **14**, 10995 (2002).
- <sup>30</sup>H. Cynn, J. E. Klepeis, C.-S. Yoo, and D. A. Young, *Phys. Rev. Lett.* **88**, 135701 (2002).
- <sup>31</sup>T. Kenichi, *Phys. Rev. B* **70**, 012101 (2004).
- <sup>32</sup>L. S. Dubrovinsky, N. A. Dubrovinskaia, V. Swamy, J. Muscat, N. M. Harrison, R. Ahuja, B. Holm, and B. Johansson, *Nature (London)* **410**, 653 (2001).

- <sup>33</sup>H.-Y. Chung, M. B. Weinberger, J. B. Levine, A. Kavner, J. M. Yang, S. H. Tolbert, and R. B. Kaner, *Science* **316**, 436 (2007).
- <sup>34</sup>D. Nishio-Hamane, A. Shimizu, R. Nakahira, K. Niwa, A. Sano-Furukawa, T. Okada, T. Yagi, and T. Kikegawa, *Phys. Chem. Miner.* **37**, 129 (2010).
- <sup>35</sup>T. S. Duffy, G. Y. Shen, D. L. Heinz, J. F. Shu, Y. Z. Ma, H. K. Mao, R. J. Hemley, and A. K. Singh, *Phys. Rev. B* **60**, 15063 (1999).
- <sup>36</sup>W. J. Nellis, G. I. Kanel, S. V. Razorenov, A. S. Savinykh, and A. M. Rajendran, *J. Phys.: Conf. Ser.* **215**, 012148 (2010).
- <sup>37</sup>A. Kubo and M. Akaogi, *Phys. Earth Planet. Inter.* **121**, 85 (2000).
- <sup>38</sup>J. R. Smyth and T. C. McCormick, in *Mineral Physics and Crystallography: A Handbook of Physical Constants*, edited by T. J. Ahrens (American Geophysical Union, Washington D. C., 1995), pp. 1–17.
- <sup>39</sup>J. Wang, Z. Mao, S. M. Dorfman, V. B. Prakapenka, and T. S. Duffy, Fall Meet. Suppl. EOS Trans. AGU **90**, Abstract MR13A (2009).
- <sup>40</sup>T. Tsuchiya, H. Yusa, and J. Tsuchiya, *Phys. Rev. B* **76**, 174108 (2007).